



Contents lists available at ScienceDirect

Journal of Nuclear Materials

journal homepage: www.elsevier.com/locate/jnucmat

Compatibility of interfaces and fibers for SiC-composites in fusion environments

C.H. Henager Jr. *, R.J. Kurtz

Pacific Northwest National Laboratory (PNNL), Materials Structure and Performance, P8-15, 902 Battelle Blvd., Richland, WA 99352, USA

A B S T R A C T

The use of SiC-composites in fusion environments is predicated on stability under neutron irradiation, on outstanding high-temperature mechanical properties, and on chemical inertness and corrosion resistance. However, SiC is susceptible to many forms of corrosion in water and in water vapor where silica formation is required as a protective layer because silica forms stable hydroxides that are volatile, even at low temperatures. SiC-composites have an additional concern that fine-grained fibers and weak interfaces provide the required fracture toughness, but these components may also exhibit susceptibility to corrosion that can compromise material properties. In this work we examine and review the compatibility of fibers and interfaces, as well as the SiC matrix, in proposed fusion environments including first wall, tritium breeding, and blanket modules and module coolants.

© 2009 Elsevier B.V. All rights reserved.

1. Introduction

SiC is an excellent material for fusion reactor environments, including first wall plasma facing materials and breeder-blanket module materials. It is low-activation, temperature-resistant, and radiation damage tolerant compared to most materials. In the form of woven or braided composites with high-strength SiC fibers it has the requisite mechanical, thermal, and electrical properties to be a useful and versatile material system for fusion applications, especially since microstructural tailoring during processing allows control over the physical properties of interest [1–11]. Chemical and environmental compatibility with fusion and blanket cooling environments appear to be positive [1,5,12,13] but uncertainties remain primarily due to inadequate testing of SiC_f/SiC materials in flowing Pb–Li and due to uncertainty in final composite architecture designs for fusion.

Although SiC is stable up to high-use temperatures, there are issues with regard to corrosion resistance and chemical reactivity of SiC that require elaboration for fusion applications. In many respects, the thorough testing of SiC/SiC in high-temperature environments has been disappointing due to the reactivity of SiC with water and water vapor, especially flowing gases. Unfortunately, this has virtually eliminated Si-based ceramics from consideration in combustion and/or engine environments. Fundamentally, Si is too reactive with hydrogen and oxygen and the formation of protective silica scales is lacking in these environments [14–24].

This paper reports on the current status of SiC and SiC-composites for fusion applications from the perspective of SiC corrosion is-

suages in water, water vapor, low-pressure oxygen, and Pb–Li. The inhomogeneous nature of SiC-composites is discussed with regard to corrosion issues of the composite materials and specifically the vulnerability of the high-strength SiC fibers and tailored interphase in the presence of matrix cracks in the SiC matrix [25,26]. It is unfortunate that limited data exists for fiber degradation as a function of fiber type so a more generic approach is taken in that regard consistent with a fine-grained, high-strength SiC fiber. Finally, the corrosion of SiC in water is not truly relevant to the fusion environment but it is used to illustrate the scope and nature of corrosion of SiC posed by other uses.

2. Corrosion of SiC

Research at NASA Lewis Research Center and at Oak Ridge National Laboratory has demonstrated the disruptive nature of water and water vapor on the protective silica film on SiC during high-temperature exposures [14,16,18–24,27]. Fig. 1 is a micrograph from the work of Tortorelli and More [22] showing the effects of water vapor on silica film morphology on α -SiC. The work at NASA [14,18–21,27] has developed the fundamental understanding of parabolic-linear oxidation of Si-based ceramics in flowing atmospheres containing water vapor. At high temperatures, SiC and Si₃N₄ react with water vapor to form a SiO₂ scale, which also reacts with water vapor to form a volatile Si(OH)₄ species. These simultaneous reactions, one forming SiO₂ and the other removing SiO₂, are described by parabolic-linear kinetics. A steady state, in which these reactions occur at the same rate, is eventually achieved, after which the oxide found on the surface is a constant thickness, and recession of the underlying material occurs at a linear rate. This data has indicated that Si-based ceramics are essentially unsuited for engine environments unless they can be coated with an

* Corresponding author. Tel.: +1 509 376 1442; fax: +1 509 376 0418.
E-mail address: chuck.henager@pnl.gov (C.H. Henager Jr.).

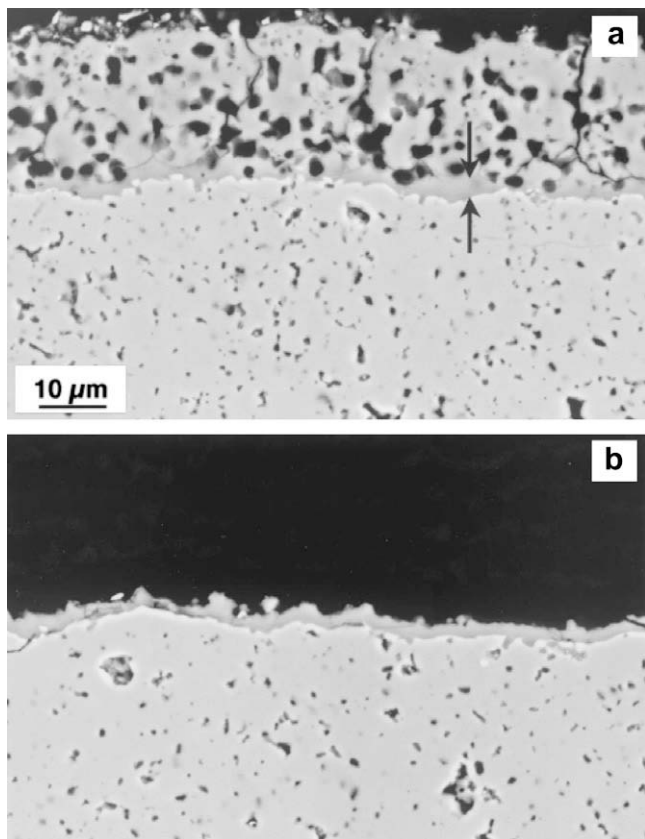


Fig. 1. SiO₂ scales on sintered α -SiC after exposure at 1200 °C for 100 h at 10 atm in (a) air 15% H₂O and (b) 100% air. Arrows in (a) denote dense vitreous SiO₂ layer [22].

environmental barrier coating. Although these chemical conditions are not truly relevant to fusion the lessons to be learned here are very relevant to the blanket module concepts that have SiC-composites in flowing liquid metal coolants, such as Pb–Li.

Recent research to understand the behavior of SiC in high-temperature water for advanced reactor concepts has shown that CVD β -SiC is prone to pitting corrosion at 573 K in deoxygenated water [28–30]. Fig. 2(a) is an SEM micrograph of a large pit observed on the surface of the CVD SiC after 2000 h of exposure. Fig. 2(b) is a compilation of the surface chemistry data obtained in the SEM using EDS methods that show the loss of Si that is observed in the pitting process. Similar chemical reactions have been suggested for the dissolution of silica in water, as are proposed for the gas phase, and which has been a topic of scientific study for some time by Tomozawa and co-workers [31–34]. Thus, silica is lost in the form of silicon hydroxides from the surface of the SiC and carbon is comparatively enriched at the surface (Fig. 3). The average Si content on the surface decreases relative to C but for the pit interiors the Si decrease is much greater making it appear that C is enriched within the pit. The form of C in the pit was not established.

3. Corrosion of SiC-composites

Unfortunately, much less information exists for SiC-composites in fusion reactor conditions, including first wall applications, tritium breeding blankets, and flow channel inserts. Reasons for this vary but include a lack of standardized material, lack of specifications for the environments, and lack of space in flowing liquid coolant test loops. Optimistically, the good news for SiC-composites is that SiC appears to be compatible with Pb–Li coolants. Pint's re-

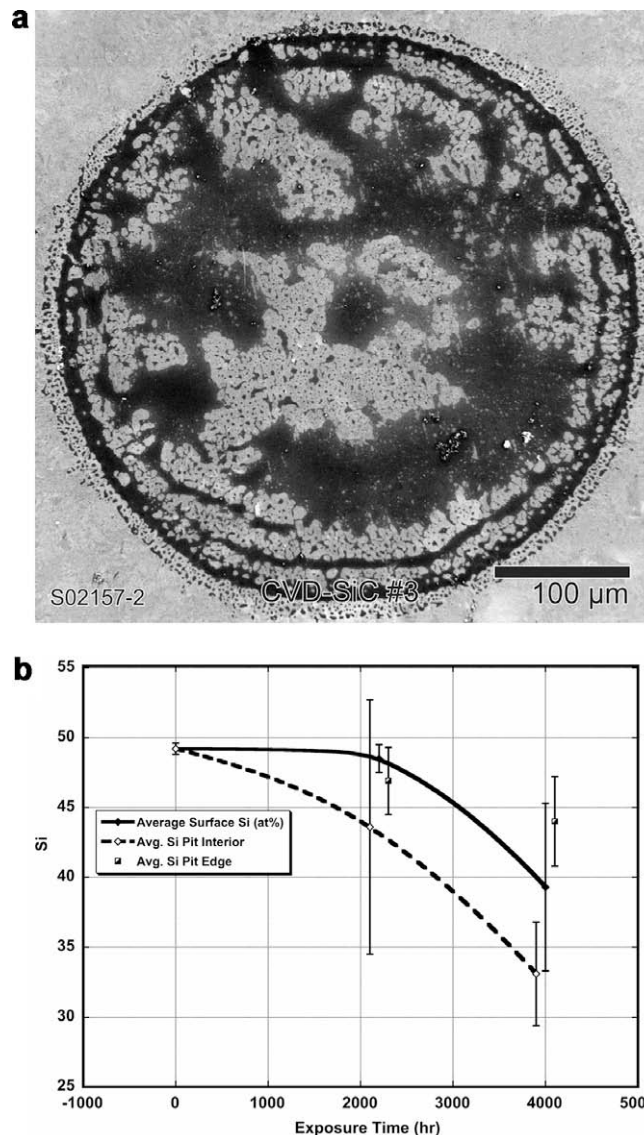


Fig. 2. (a) SEM images of large pit showing complex fractal-like pit morphology and (b) plot of average Si composition in atomic % as a function of time and location on the surface of the CVD SiC. The data points have been shifted slightly along the x-axis (time) for clarity.

search with β -SiC helps establish the compatibility of SiC with Pb–Li coolants below 1373 K [1], while studies by Yoneoka et al. [35] and Barbier et al. [36] suggest that SiC-composites also have little interaction with Pb–Li coolants. However, this data is preliminary and only involves static exposures, not flowing. Pint discusses concerns regarding fiber and interphase corrosion and the need for a seal coating [1]. This is also suggested by the work of Barbier where Pb–Li ingress into voids in the SiC-composite was observed [36], which suggests wetting of the SiC by the Pb–Li liquid occurs during exposure.

Even with a seal coating, the conservative approach is to consider a cracked seal coat and Pb–Li ingress to the SiC-composite. We consider the corrosion issues with a SiC_f/SiC composite consisting of a fine-grained SiC fiber, such as the Hi-Nicalon Type-S fiber, and a pyrocarbon interphase. Without specific degradation data in Pb–Li environments, a time-dependent bridging model is useful to understand fiber and fiber/matrix interphase degradation. The degradation mechanisms of Type-S SiC fibers are thermal creep cavitation causing stress rupture [37] and irradiation creep, and these

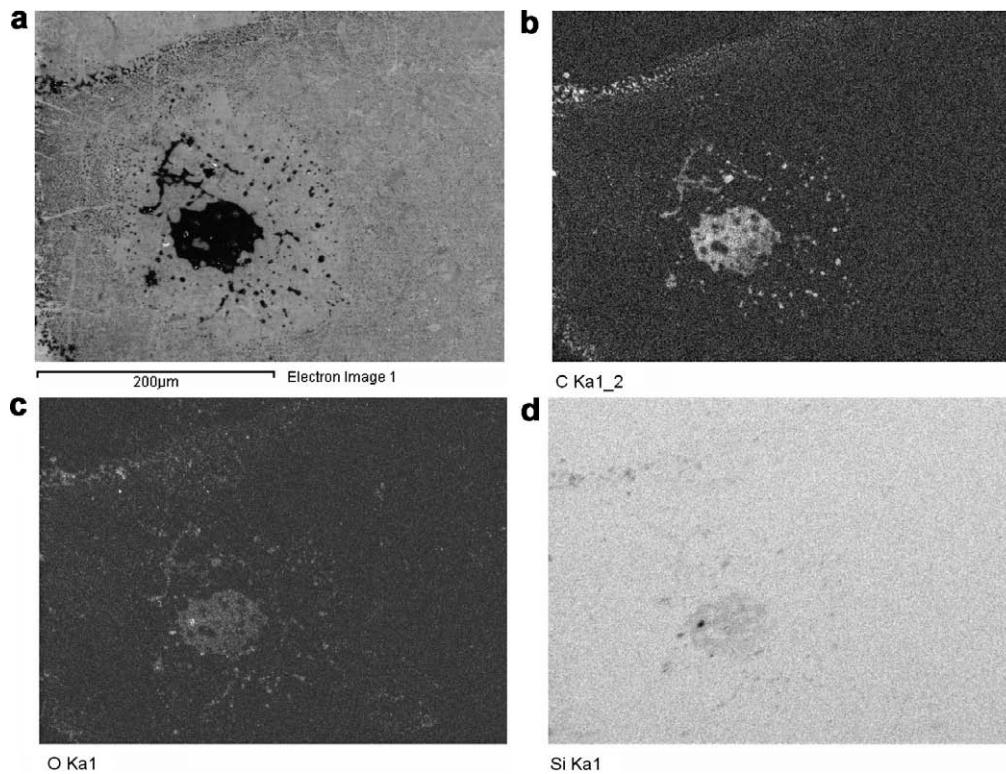


Fig. 3. SEM image and X-ray map images of a pit on a 2000-h exposed sample of β -SiC. The image in (a) can be directly correlated with the associated element maps shown in (b–d). The carbon map is shown in (b), the oxygen map in (c) and the silicon map in (d). The pit is enriched in C and O relative to the matrix and depleted in Si.

processes have been treated in prior studies [38]. For the current study, a static bridging model was developed based on the dynamic model physics [39,40]. We consider fiber strength reductions and fiber/matrix degradation due to environmental damage in first wall and breeder-blanket applications.

The model is calibrated using single-edge-notched beam (SENB) data for a five-harness satin weave, 0/90 Type-S fiber, CVI-SiC-composite manufactured by GE Power Systems,¹ which has a peak load fracture toughness of $K_{Q} = 22.9 \text{ MPa}\sqrt{\text{m}}$ at ambient temperature and an ultimate strength in four-point bending of 750 MPa [41]. The PNNL time-dependent crack bridging model can be used to estimate fracture loads of SiC_f/SiC in SENB geometries that depend on fiber strength and interphase properties. Table 1 lists the model input parameters and the model indicates that if the fiber fracture strength is assumed to be 2.5 GPa that a good agreement with measured K_{Q} is achieved for an interfacial shear strength value of 15 MPa. The use of the K_{Q} values is understood to be a qualitative measure of fracture toughness for these materials as defined in ASTM E399-90 [42]. A recent discussion of fracture toughness measurements in composites points out the difficulties in these measurements [43].

We examine the effect of loss of fiber strength due to an unspecified interaction with a corrosive liquid or gas. The results of this are presented in Fig. 4 and show that a loss of fiber strength from 2.5 GPa to 1.85 GPa will reduce the SiC-composite toughness to an unacceptable level. Based on fiber creep data for the Type-S fiber we can calculate the approximate time to reach 1% creep strain at 1073 K to be in excess of 5×10^5 h, which drops to about 12,000 at 1173 K and only 400 h at 1273 K. This assumes the existence of a bridged crack in the composite under a moderate load. Operation at 800 °C or 1073 K would assure a long lifetime with respect to creep rupture only if no significant fiber degradation due

Table 1

Parameters for static and dynamic bridging model.

Parameter	Value
SENB width	5.5 mm
SENB notch length	1.0 mm
CVI-SiC modulus	$4.6 \times 10^5 \text{ MPa}$
Hi-Nicalon Type-S SiC fiber modulus	$4.2 \times 10^5 \text{ MPa}$
Composite modulus	$1.81 \times 10^5 \text{ MPa}$
Bridging fiber volume fraction	0.2
Fiber radius	7 μm
Interfacial shear stress (τ)	15 MPa
Fiber fracture strength	2500 MPa

to the fusion environment occurs. Thus, flowing Pb–Li tests on SiC fibers are required to demonstrate that no degradation occurs over thousands of hours.

The second parametric study is an interaction between the environment and the fiber/matrix interphase. This is problematic since the interphase that will be selected is not known so we assume a thin pyrocarbon interphase with interfacial shear strength of 15 MPa as suggested by the bridging model. We consider interactions between the environment and the interphase that cause an increase in bonding [44–51] and use the static bridging model to calculate fracture toughness due to changes in the interfacial shear strength. Fig. 5 shows that if the interfacial shear strength is increased from 15 MPa to above 40 MPa the composite fracture toughness will fall below the acceptable limit of $15 \text{ MPa}\sqrt{\text{m}}$. Thus, the fiber/matrix interphase materials must also be unaffected and this may represent the most vulnerable part of the SiC/SiC composite material system. This result suggests that tests in flowing Pb–Li be coordinated with post-test fracture toughness measurements on composite materials.

The final parametric study involves an area that has been previously address by the dynamic bridging model when oxidation

¹ <http://www.gepower.com>.

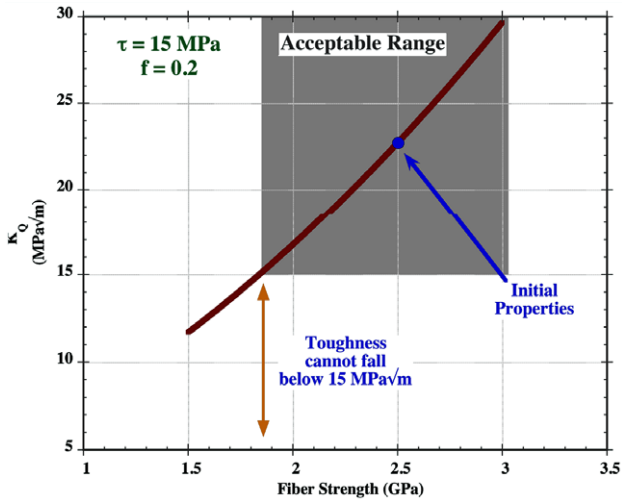


Fig. 4. Parametric plot of SiC-composite fracture toughness as a function of fiber fracture strength. This plot illustrates the decrease in fracture toughness expected due to a loss of fiber strength due to corrosion or environmental degradation.

removal of a thin carbon interphase was treated, which is relevant for fusion first wall exposures and low-oxygen partial pressures or volatilization reactions in flowing Pb–Li in blanket modules. Interphase removal due to chemical reactions causes a decrease in bridging effectiveness and loss of crack growth resistance. These calculations are performed using the dynamic crack bridging model and allowing the oxidation of the thin pyrocarbon interface to proceed in order to simulate a volatile reaction. These results are shown in Fig. 6 and illustrate the large effect of even very small recession rates. A recession rate at the interface of 3×10^{-9} m/s can cause an additional crack extension of 1-mm over 1 year for a hypothetical bridged crack in SiC/SiC, which may be unacceptable. Such issues will require greater knowledge of component design and operating parameters than is presently available.

The implications of this survey and parametric study for SiC-composites for fusion are relatively obvious at this stage. In order to prevent a critical loss of strength and toughness, the environment can degrade neither the fiber nor the fiber–matrix interphase. For stressed components and structural members this is absolutely critical but for parts of the tritium breeding or cooling

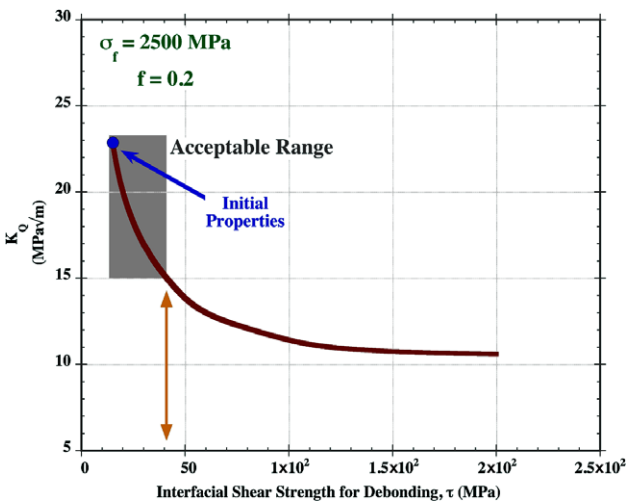


Fig. 5. Composite fracture toughness as a function of interfacial shear strength for debonding, τ , showing the loss of toughness due to an increased shear strength such as oxidation embrittlement reactions at the interface.

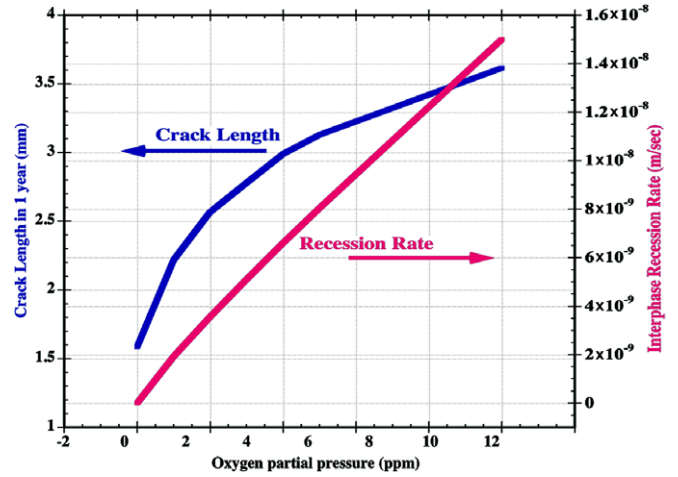


Fig. 6. Crack extension in addition to that due to fiber creep during 1-year operation due to recession of fiber/matrix interphase, which here is reaction of pyrocarbon with oxygen at 1373 K. This parametric plot illustrates the sensitivity of a bridged crack to interphase removal due to volatilization.

system, such as a SiC/SiC flow channel insert that does not carry load, this is less critical. In that case overall corrosion rates in flowing Pb–Li are more important. Fusion first wall applications gaseous corrosion and oxygen content in the plasma is critical to those corrosion rates. Without additional data or environmental operation conditions it is difficult to be more precise.

4. Conclusions

The most important conclusion from this overview study of compatibility issues for SiC-composites in fusion environments is that there is a critical lack of data for SiC-composites in flowing Pb–Li environments. Notwithstanding the apparent unreactivity of SiC and SiC/SiC with Pb–Li in static tests, this paper has pointed out the complexity of the SiC/SiC material system with a CVI-matrix, a fine-grained, high-strength fiber, and a weak, debonding fiber/matrix interphase, which raises concerns for the behavior of this system in a potentially corrosive environment. Fortunately, SiC appears to be compatible with Pb–Li but this needs to be verified in flowing environments. The fibers and fibers coated with typical interphase materials also need to be studied in this manner. Finally, SiC/SiC-composites need to be exposed in flowing Pb–Li and post-test retained strength or retained fracture toughness measured. The evidence that Pb–Li collects within the pores of uncoated SiC/SiC is of some concern at this point but further tests are required. The use of mechanical property modeling, as used here, can guide the experimentation and establish needed confidence levels for the research.

Acknowledgements

PNNL is operated for the US Department of Energy by Battelle Memorial Institute under Contract DE-AC06-76RLO 1830.

References

- [1] B.A. Pint, J.L. Moser, P.F. Tortorelli, J. Nucl. Mater. 367–370 (2007) 1150.
- [2] Y. Katoh, L.L. Snead, C.H. Henager Jr., A. Hasegawa, A. Kohyama, B. Riccardi, H. Hegeman, J. Nucl. Mater. 367–370A (2007) 659.
- [3] C.H. Henagers Jr., Y. Shin, Y. Blum, L.A. Giannuzzi, B.W. Kempshall, S.M. Schwarz, J. Nucl. Mater. 367–370 (2007) 1139.
- [4] S.J. Zinkle, Fus. Eng. Des. 74 (2005) 31.
- [5] B.A. Pint, K.L. More, H.M. Meyer, J.R. DiStefano, Fus. Sci. Technol. 47 (2005) 851.
- [6] J.B.J. Hegeman, J.G. Van Der Laan, M. Van Kranenburg, M. Jong, D. D’Hulst, P. Ten Pierick, Fus. Eng. Des. 75–79 (2005) 789.
- [7] J. Sha, A. Kohyama, Y. Katoh, Plasma Sci. Technol. 5 (5) (2003) 1965.

- [8] B.A. Pint, J.R. DiStefano, P.F. Tortorelli, *Fus. Sci. Technol.* 44 (2003) 433.
- [9] Y. Katoh, A. Kohyama, T. Hinoki, L.L. Snead, *Fus. Sci. Technol.* 44 (2003) 155.
- [10] R.H. Jones, L. Giancarli, A. Hasegawa, Y. Katoh, A. Kohyama, B. Riccardi, L.L. Snead, W.J. Weber, *J. Nucl. Mater.* 307–311 (2002) 1057.
- [11] Y. Katoh, T. Nozawa, L.L. Snead, T. Hinoki, A. Kohyama, *Fus. Eng. Des.* 81 (2006) 937.
- [12] C.P.C. Wong, S. Malang, M. Sawan, M. Dagher, S. Smolentsev, B. Merrill, M. Youssef, S. Reyes, D.K. Sze, N.B. Morley, S. Sharafat, P. Calderoni, G. Sviatoslavsky, R. Kurtz, P. Fogarty, S. Zinkle, M. Abdou, *Fus. Eng. Des.* 81 (2006) 461.
- [13] C.P.C. Wong, S. Malang, M. Sawan, S. Smolentsev, S. Majumdar, B. Merrill, D.K. Sze, N. Morley, S. Sharafat, M. Dagher, P. Peterson, H. Zhao, S.J. Zinkle, M. Abdou, M. Youssef, *Fus. Sci. Technol.* 47 (2005) 502.
- [14] N. Jacobson, D. Myers, E. Opila, E. Copland, *J. Phys. Chem. Solids* 66 (2005) 471.
- [15] Q.N. Nguyen, E.J. Opila, R.C. Robinson, *J. Electrochem. Soc.* 151 (2004) 558.
- [16] E.J. Opila, *J. Am. Ceram. Soc.* 86 (2003) 1238.
- [17] S.R. Levine, E.J. Opila, M.C. Halbig, J.D. Kiser, M. Singh, J.A. Salem, *J. Eur. Ceram. Soc.* 22 (2002) 2757.
- [18] D.S. Fox, E.J. Opila, R.E. Hann, *J. Am. Ceram. Soc.* 83 (2000) 1761.
- [19] E.J. Opila, *J. Am. Ceram. Soc.* 82 (1999) 625.
- [20] E.J. Opila, R.E. Hann Jr., *J. Am. Ceram. Soc.* 80 (1997) 197.
- [21] N.S. Jacobson, E.J. Opila, D.S. Fox, J.L. Smialek, *Mater. Sci. Forum* 251–254 (1997) 817.
- [22] P.F. Tortorelli, K.L. More, *J. Am. Ceram. Soc.* 86 (2003) 1249.
- [23] K.L. More, P.F. Tortorelli, L.R. Walker, N. Miriyala, J.R. Price, M. Van Roode, *J. Am. Ceram. Soc.* 86 (2003) 1272.
- [24] K.L. More, P.F. Tortorelli, M.K. Ferber, J.R. Keiser, *J. Am. Ceram. Soc.* 83 (2000) 211.
- [25] R.H. Jones, C.H. Henager Jr., *J. Eur. Ceram. Soc.* 25 (2005) 1717.
- [26] C.H. Henager Jr., E.A. Le, R.H. Jones, *J. Nucl. Mater.* 329–333 (2004) 502.
- [27] E. Opila, *Ceram. Eng. Sci. Proc.* 26 (2005) 311.
- [28] C.H. Henager Jr., A.L. Schemer-Kohn, S.G. Pitman, D.J. Senior, K.J. Geelhood, C.L. Painter, *J. Nucl. Mater.* 378 (2008) 9.
- [29] E. Barringer, Z. Faiztompkins, H. Feinroth, T. Allen, M. Lance, H. Meyer, L. Walker, E. Lara-Curzio, *J. Am. Ceram. Soc.* 90 (2007) 315.
- [30] W.-J. Kim, H.S. Hwang, J.Y. Park, W.-S. Ryu, *J. Mater. Sci. Lett.* 22 (2003) 581.
- [31] A. Oehler, M. Tomozawa, *J. Non-Cryst. Solids* 347 (2004) 211.
- [32] M. Tomozawa, *Phys. Chem. Glasses* 39 (1998) 65.
- [33] M. Nogami, M. Tomozawa, *J. Am. Ceram. Soc.* 67 (1984) 151.
- [34] S. Ito, M. Tomozawa, *J. Am. Ceram. Soc.* 64 (1981) C/160.
- [35] T. Yoneoka, S. Tanaka, T. Terai, *Mater. Trans.* 42 (2001) 1019.
- [36] F. Barbier, P. Deloffre, A. Terlain, *J. Nucl. Mater.* 307–311 (2002) 1351.
- [37] J.A. DiCarlo, H.M. Yun, J.B. Hurst, *Appl. Math. Comput. (New York)* 152 (2004) 473.
- [38] C.H. Henager Jr., *J. Nucl. Mater.* 367–370A (2007) 742.
- [39] C.H. Henager Jr., C.A. Lewinsohn, R.H. Jones, *Acta Mater.* 49 (2001) 3727.
- [40] C.H. Henager Jr., R.G. Hoagland, *Acta Mater.* 49 (2001) 3739.
- [41] C. Henager Jr., in: S. Marra (Ed.), *Ceramics in Nuclear and Alternative Energy Applications*, John Wiley, 2006, p. 127.
- [42] ASTM, ASTM E 399–90, *Standard Test Method for Plane-Strain Fracture Toughness, Fracture Toughness of Metallic Materials* (ASTM, 1997).
- [43] R.C. Petersen, J.E. Lemons, M.S. McCracken, *Polym. Compos.* 28 (2007) 311.
- [44] C.A. Lewinsohn, G.E. Youngblood, C.H. Henager Jr., E.P. Simonen, R.H. Jones, *J. Nucl. Mater.* 283–287 (2000) 584.
- [45] G.N. Morscher, J. Martinez-Fernandez, *Adv. Sci. Technol.* 22 (1999) 331.
- [46] T.E. Steyer, F.W. Zok, D.P. Walls, *J. Am. Ceram. Soc.* 81 (1998) 2140.
- [47] C.A. Lewinsohn, C.H. Henager Jr., R.H. Jones, *Ceram. Eng. Sci. Proc.* 19 (1998) 11.
- [48] M.J. Verrilli, A.M. Calomino, D.N. Brewer, *ASTM Spec. Tech. Publ. STP 1309* (1997) 158.
- [49] H.-T. Lin, P.F. Becher, *Composites Part A* 28A (1997) 935.
- [50] A.G. Evans, F.W. Zok, R.M. McMeeking, Z.Z. Du, *J. Am. Ceram. Soc.* 79 (1996) 2345.
- [51] R. Kahraman, J.F. Mandell, M.C. Deibert, *J. Mater. Sci.* 30 (1995) 6329.